HHS Public Access

Author manuscript

Genes Chromosomes Cancer. Author manuscript; available in PMC 2022 December 01.

Published in final edited form as:

Genes Chromosomes Cancer. 2021 December ; 60(12): 796–807. doi:10.1002/gcc.22992.

Recurrent loss of chromosome 22 and *SMARCB1* deletion in extra-axial Chordoma: A clinicopathological and molecular analysis

Xiaoyun Wen, MD, PhD[1], **Robert Cimera**[1], **Ruth Aryeequaye**[1], **Mohanty Abhinta**[1], **Edward Athanasian, MD**[2], **John Healey, MD**[2], **Nicola Fabbri, MD**[2], **Patrick Boland, MD**[2], **Yanming Zhang, MD, PhD**[1], **Meera Hameed, MD**[1,*]

[1]Department of Pathology, Memorial Sloan Kettering Cancer Center, New York, NY

[2]Department of Surgery, Memorial Sloan Kettering Cancer Center, New York, NY

Abstract

Extra-axial chordoma is a rare neoplasm of extra-axial skeleton and soft tissue that shares identical histomorphologic and immunophenotypic features with midline chordoma. While genetic changes in conventional chordoma have been well-studied, the genomic alterations of extra-axial chordoma have not been reported. It is well known that conventional chordoma is a tumor with predominantly non-random copy number alterations and low mutational burden. Herein we describe the clinicopathologic and genomic characteristics of six cases of extra-axial chordoma, with genome-wide high-resolution single nucleotide polymorphism array, fluorescence in situ hybridization and targeted next-generation sequencing (NGS) analysis. The patients presented at a mean age of 33 years (range: 21-54) with a female to male ratio of 5:1. Four cases were histologically conventional type, presented with bone lesions and three of them had local recurrence. Two cases were poorly differentiated chordomas, presented with intra-articular soft tissue masses and both developed distant metastases. All cases showed brachyury positivity and the two poorly differentiated chordomas showed in addition loss of INI-1 expression by immunohistochemical analysis. Three of four extra-axial conventional chordomas showed simple genome with loss of chromosome 22 or a heterozygous deletion of *SMARCB1*. Both poorly differentiated chordomas demonstrated a complex hyperdiploid genomic profile with gain of multiple chromosomes and homozygous deletion of *SMARCB1*. Our findings show that heterozygous deletion of *SMARCB1* or the loss of chromosome 22 is a consistent abnormality in extra-axial chordoma and transformation to poorly differentiated chordoma is characterized by homozygous loss of *SMARCB1* associated with genomic complexity and instability such as hyperdiploidy.

Keywords

Extra-axial chordoma; extra-axial poorly differentiated chordoma; INI1; *SMARCB1*

[*]Corresponding author: Meera Hameed MD, Department of Pathology, Memorial Sloan Kettering Cancer Center, 1275 York Avenue, New York, NY 10065, USA. Phone: 212-639-5905, hameedm@mskcc.org, Fax: 212-772-8521.

Disclosure/conflict of interest

The authors declare no conflict of interest.

Introduction

Chordoma is a rare slow growing, locally aggressive malignant bone tumor with metastases occurring in about 40% of the cases. It is believed to arise from embryonic remnants of notochord and thus exclusively occur in the axial skeleton with a predilection for the sacrococcygeal region (50%), the base of the skull near the spheno-occipital area (35%) and the vertebral bodies (15%) [1]. There are four histological subtypes of chordoma: conventional, chondroid, dedifferentiated and poorly differentiated [2].

Extra-axial chordoma is extremely rare and arises in the extra-axial skeleton and soft tissue. While axial chordoma can be construed to be arising from notochordal remnants, the origin of extra-axial chordoma is unknown. An undifferentiated pluripotent stem cell with an ability to differentiate into notochordal lineage remains a possibility [3]. Chordoma and extra-axial chordoma share identical morphologic and immunophenotypic features. Both tumors are composed of epithelioid cells with variably vacuolated and bubbly eosinophilic cytoplasm (so-called “physaliphorous” cells) embedded in a myxoid background and show co-expression of keratins, S100 and universal nuclear positivity for brachyury which is a highly specific marker of notochord differentiation [4]. Poorly differentiated chordoma is a rare subtype of axial chordoma with a poor prognosis. Histologically, poorly differentiated chordomas show epithelioid cells with rhabdoid morphology, higher grade cytological features with positivity for brachyury and loss of INI-1 expression, related to *SMARCB1* associated genetic alterations [5-7].

Genetic studies have demonstrated that conventional chordomas are tumors with very low to modest mutation burden and are predominantly characterized by large copy number losses, typically involving chromosomes/chromosomal arms 1p, 3, 9q, 10, 13 and 14 and a small number of arm or chromosome gains of 7 and 1q [6,8,9]. In a large study of 104 cases of sporadic chordomas, PI3K signaling pathway mutations were seen in 16% of the cases [10]. The genomic complexity increases as the tumor progresses from conventional chordoma to dedifferentiated chordoma [11]. Poorly differentiated chordoma, on the other hand, is more prevalent in pediatric and young adult patients and typically demonstrates inactivating mutations and /or homozygous deletion involving the *SMARCB1* gene at 22q11.23 [5-7].

The genetic alterations of extra-axial chordoma have not been reported thus far. Herein we report the clinical and pathologic features of 6 cases of extra-axial chordoma, and utilized genome-wide high-resolution single nucleotide polymorphism (SNP)-Array, fluorescence in situ hybridization (FISH) and targeted next-generation sequencing (NGS) to analyze copy number changes, allelic imbalances, and mutations in this very rare subtype of chordoma.

Materials and Methods

Patient Data and Tumor Specimens:

The study was conducted with institutional Review Board approval (IRB#17-067) and included 6 retrospectively identified patients (5 in-house cases and 1 departmental consultation case) who were diagnosed as extra-axial chordoma during 2006 to 2020 at

our institution. Two cases (case number 3 and 4) were previously reported as case reports [12]. None of the patients in this cohort had history or diagnosis of axial chordoma or benign notochordal cell tumor. Follow-up data were available for all 6 patients up to 174 months (14.5 years). The histological slides were reviewed by 2 pathologists (one subspecialized bone and soft tissue pathologist). 4 cases with adequate tumor content (overall tumor content: >70%) were subjected to SNP-array and FISH analysis, and 2 cases without adequate tumor content were subjected to FISH analysis for *SMARCB1* gene deletion. Next-generation sequencing data was available for 3 patients. The clinical information for all patients was obtained through manual review of electronic medical record.

Immunohistochemical staining:

The immunohistochemical stains were performed at the Department of Pathology, MSKCC, using commercially available antibodies. Staining for pan-cytokeratin (clone AE1/AE3, Dako, 1:1600), EMA (clone E29, Ventana, pre-diluted), S100 (polyclonal, Dako, 1:8000), INI-1/BAF-47 (clone 25/BAF47, BD Bioscience, 1:200) were performed on the automated Ventana BenchMark ULTRA immunostainer (Roche, Indianapolis, IN), using OptiView DAB IHC Detection Kit (Ventana Medical Systems, Tucson, AZ). Staining for Brachyury (clone EPR18113, Abcam, 1:500) was performed on the Leica Bond-3 immunostainer (Leica, Buffalo Grove, IL), using a polymer detection system (DS9800; Leica, Bond Polymer Refine Detection).

SNP-array analysis:

Genomic DNA was extracted from formalin-fixed and paraffin-embedded (FFPE) tumor tissues using a magnetic bead-based chemagic FFPE DNA kit (PerkinElmer, Waltham, MA) on a Hamilton chemagic STAR liquid handling system (Hamilton Company, Reno, NV) according to the manufacturer's instructions. Genome-wide DNA copy number alterations and allelic imbalances were analyzed by OncoScan CNV assay (Thermo Fisher Scientific, Waltham, MA) using 80 ng of genomic DNA for each sample according to the manufacturer's instructions. OncoScan SNP-assay data were analyzed by OncoScan Console ChAS 4.0 software (Thermo Fisher Scientific, Waltham, MA) and Nexus Copy Number 10 software (BioDiscovery, El Segundo, CA) using Affymetrix TuScan algorithm (Thermo Fisher Scientific, Waltham, MA). All SNP-array data were also manually reviewed for subtle alterations not automatically called by the software.

FISH analysis:

Formalin-fixed, paraffin-embedded, 4 μm thick tissue sections with tumor areas marked were used for FISH analysis following standard protocols. To confirm homozygous deletions of *SMARCB1* gene revealed by SNP array analysis, FISH probe for *SMARCB1* (22q11.23) (Agilent, Santa Clara, California) in combination with an internal control probe (22q11.12) (Empire Genomics, Williamsville, New York) was used. Signal analysis was performed in combination with morphology correlation, and 100 interphase cells within the marked tumor area were evaluated and imaged using a ZEISS fluorescence microscope (ZEISS, Oberkochen, Germany) coupled with MetaSystems ISIS software (MetaSystems, Altlußheim, Germany).

NGS-targeted sequencing:

Genomic DNA was extracted from formalin-fixed and paraffin-embedded (FFPE) tumor tissues and were screened for gene mutations in 468 key cancer-associated genes using solution-phase exon capture and next-generation sequencing (NGS) as previously described (MSK-IMPACT, MSK-Integrated Mutation Profiling of Actionable Cancer Targets) [13].

Results

Clinical data:

The clinicopathologic features of 6 cases of extra-axial chordoma are summarized in table 1. These include four cases of extra-axial conventional chordoma (case number 1 to 4) and two cases of extra-axial poorly differentiated chordoma characterized by brachyury positivity and loss of INI-1 expression (case number 5 and 6). All patients were adults with a mean age of 33 (range of 21-54 years) and the female to male patient ratio was 5:1. The main clinical symptoms were pain and/or swelling. Among the four extra-axial conventional chordoma cases, two were intra-medullary lytic lesions (proximal humerus (Fig. 1A-B) and middle phalanx of right middle finger) and two were intra-cortical lytic lesions (distal tibia and distal femur). Both extra-axial poorly differentiated chordoma cases were intra-articular soft issue masses (elbow and knee). The size of the four extra-axial conventional chordomas ranged from 1.5 to 5.1 cm while the two extra-axial poorly differentiated chordomas ranged in size from 7.8 to 15.4 cm. Three patients with extra-axial conventional chordoma had local recurrence at 2.5 years, 8 months, and 2 years, respectively, after the initial treatment with marginal excision/curettage (case number 2, 3 and 4). None of the patients with extra-axial conventional chordoma had local recurrence or distant metastases after resection with negative margins (case number 1, 2 and 3) or a second marginal excision/curettage (case number 4). However, the two extra-axial poorly differentiated chordoma patients had developed distant metastases. One of these two patients (case number 5) was found to have metastatic disease to pleura and mediastinal lymph nodes at the time of primary diagnosis and underwent chemotherapy. The other patient (case number 6) developed metastatic disease to the inguinal lymph node, rib and pleura at 3 months, 8 months and 14 months, respectively, after radical resection, and this patient received post-operative chemotherapy and local radiation therapy. At the time of last follow up (range 7-174 months), four patients with extra-axial conventional chordoma are alive with no evidence of disease (range 32-174 months), and two patients with extra-axial poorly differentiated chordoma are alive with disease (at 7 months and 21 months, respectively). Two cases (case number 3 and 4) have been previously published as a case report without accompanying genetic analysis [12].

Pathology:

Grossly, one of the resected extra-axial conventional chordoma from the humerus showed intramedullary well-circumscribed lobulated white nodules with glistening cut surface (Fig. 1A). The poorly differentiated extra-axial chordoma where a resection specimen was available, revealed a large intra-articular mass involving deep soft tissues with white tan, nodular, solid to focal myxoid cut surface and focal necrosis (Fig. 1B). Histological features of the four extra-axial conventional chordomas showed epithelioid cells with variably vacuolated clear to eosinophilic cytoplasm organized in sheets, cords or nests in an abundant

extracellular myxoid matrix with a lobular growth pattern (Fig. 2A-B). All four cases displayed minimal to mild cytologic atypia and low to moderate cellularity without mitosis and necrosis. Immunohistochemical analysis confirmed that all four cases had diffuse nuclear staining for brachyury (Fig. 2C), focal to patchy staining for pan-cytokeratin (pan-CK) and epithelial membrane antigen (EMA), focal staining for S-100 protein and retained nuclear expression of INI-1 (Fig. 2D) with one case showing partial loss. The two extra-axial poorly differentiated chordomas were composed of two components, one showing epithelioid cells with partially vacuolated clear to eosinophilic cytoplasm organized in cords or nests in an abundant extracellular myxoid matrix (Fig. 3B), similar to conventional chordoma, and a second component showing solid sheets of poorly differentiated epithelioid to rhabdoid cells with nuclear pleomorphism, prominent nucleoli and abundant eosinophilic cytoplasm and no extracellular myxoid stroma (Fig. 3A). In the poorly differentiated component, mitoses were frequent (up to 27 mitotic figures per 10 high-power fields) and focal tumor necrosis was present. Immunohistochemical analysis in both cases showed diffuse positivity for brachyury (Fig. 3C-D), pan-CK, EMA, and uniform loss of INI-1 nuclear expression in both the conventional and poorly differentiated components indicative of loss of function of *SMARCB1* gene (Fig. 3E-F).

SNP Array Analysis, FISH Validation and NGS-targeted Sequencing:

Oncoscan array analysis was performed in four of six patients with available tissue or DNA resources. Two of these were extra-axial conventional chordomas and two were extra-axial poorly differentiated chordomas. Array analysis of the extra-axial conventional chordomas (case number 1 and 2) detected very few genomic imbalances with loss of chromosome 22 homologue in both patients, and additionally loss of chromosome 9 in case number 1 (Fig. 4A) and gain of 4q in case number 2. In contrast, a complex hyperdiploid genomic profile was observed in both patients with poorly differentiated chordoma, one (case number 5) with gain of chromosomes or chromosomal arms 1q, 7, 8q, and 18, CN-LOH of chromosome 2 and loss of 8p and segment 22q11.21-q12.2 (Fig. 5A), and the other (case number 6) with gain of chromosomes or chromosomal arms 2, 5q, 7, 8, 11, 12, 13, 14, 20 and 22. Strikingly, heterozygous or homozygous deletion involving the *SMARCB1* gene at 22q11.2 was observed in all four patients, with homozygous deletion in both patients with poorly differentiated chordoma, and in one patient with conventional chordoma (case number 1) as a subclone. In case number 6 while there was a gain of ch22, there was also a homozygous deletion of *SMARCB1* locus. Moreover, the relationship and evolution of genomic abnormalities from conventional chordoma to poorly differentiated chordoma was also demonstrated in case number 6 which had both conventional and poorly differentiated components. In case number 6, SNP-array analysis of a macrodissected focus with conventional chordoma morphology detected only focal heterozygous deletion of 22q including *SMARCB1* without any other genomic alterations, whereas the poorly differentiated chordoma component showed a complex hyperdiploid genomic profile with gain of multiple chromosomes and a homozygous deletion of *SMARCB1*, indicating genomic evolution of poorly differentiated chordoma in this case is characterized by homozygous deletion of *SMARCB1* followed by genomic complexity and instability such as hyperdiploidy (Fig. 6A).

FISH analysis using *SMARCB1* probe in combination with an internal control probe near the centromere region of chromosome 22 confirmed a homozygous deletion of *SMARCB1* in both patients with extra-axial poorly differentiated chordoma (Fig. 5B and 6B). In case number 1 and 2, with extra-axial conventional chordoma, FISH analysis confirmed loss of *SMARCB1* and the control probe, consistent with heterozygous loss of chromosome 22 (Fig. 4B), revealed by oncoscan SNP array analysis. Additionally, in case number 1, FISH also detected a small subclone with polysomy of chromosome 22. In the two patients with no array results, FISH analysis showed heterozygous *SMARCB1* deletion in one case (case number 3) and the second case (case number 4) showed about 10-15% of the cells with heterozygous deletion of *SMARCB1* which is below our FISH cut-off for deletion (30%). This was a biopsy specimen and the resected material was not available for further studies. Overall, five out of six (83%) cases of extra-axial chordomas showed *SMARCB1* deletion either by array or FISH or both with homozygous deletion of *SMARCB1* in the two cases of poorly differentiated chordomas (table 2).

NGS-targeted sequencing by MSK-IMPACT was available in three of six patients. One was extra-axial conventional chordomas (case number 1) and two were extra-axial poorly differentiated chordomas (case number 5 and 6). NGS-targeted sequencing confirmed a heterozygous deletion of *SMARCB1* in the patient with extra-axial conventional chordoma (case number 1) and homozygous deletion of *SMARCB1* in both patients with extra-axial poorly differentiated chordoma (case number 5 and 6). No mutations or structural variants were identified in any of these three cases. No copy number alterations were detected in case number 1 and the gain of chromosomes or chromosomal arms 2, 5q, 7, 8, 11, 12, 13, 14, 20 and 22 was confirmed in case number 6 by NGS-targeted sequencing. The copy number alterations in case number 5 could not be evaluated due to high background noise.

Discussion

Extra-axial chordomas are uncommon neoplasms of the extra-axial skeleton and soft tissue. Historically, this group of lesions with similar morphology to chordoma were referred as “parachordoma” and included tumors of myoepithelial origin, extraskeletal myxoid chondrosarcoma and chordoma [14].This histological conundrum was put to rest after the identification of brachyury belonging to the T-box transcription factor family as a highly specific marker for notochord differentiation, thus enabling an accurate diagnosis of extra-axial chordoma [4]. The term “parachordoma” has been largely abandoned and tumors with morphological resemblance to chordoma as above and metastatic carcinomas can be readily distinguished by absence of brachyury expression and other immunohistochemical and molecular findings [15]. To date, 17 publications with a total of 26 brachyury-positive extra-axial chordoma cases have been reported in the English-language literature, most of them as case reports and one case series comprising 6 extra-axial chordoma cases [3,12,15-29]. In these cases, the gross and microscopic appearance, immunohistochemical phenotype and clinical course of the extra-axial chordoma were identical to those of a midline chordoma, except that extra-axial chordoma can occur at younger ages. While karyotyping has shown loss of chromosome 22 in a case of parachordoma [30], to the best of our knowledge, there have been no SNP array analysis describing genetic alterations in extra-axial chordoma thus far.

The genomic characteristics of axial conventional chordomas have been well studied by various analyses with methodologies which included SNP array, targeted next-generation sequencing, whole exome (WES) and whole genome sequencing (WGS) [6,8-10,31-35]. Several studies have shown that chordoma is a tumor with low mutation burden and belong to C-class oncogenic signature with copy number losses as primary genetic events [6,8,9,36] and few cases showing duplication of 6q27 where T-box transcription factor gene, brachyury is located [33-35,37]. Most commonly involved copy number changes include losses of 1p,3, 9p,10,13 and 14 [9]. Recurrent somatic mutations as reported by WGS and WES studies include mutations in PI3K signaling pathway genes in 16% (*PIk3CA*, *PTEN*, *PIK3R1*), chromatin remodeling genes in 17% (*ARID1A*, *PBRM1*, *SETD2*), recurrent truncating mutations in LYST, a lysosomal trafficking protein in 10% [10]. It is to be noted both *SETD2* and *PBRM1* are located at ch3p which is a common region for chromosomal loss (LOH) in chordoma [9]. Additionally, *CDKN2A* located at ch9p is one of the frequently inactivated genes in chordoma [38]. In about 20% of cases chromothripsis can be observed on SNP array or WGS (whole genome sequencing) and often involves multiple chromosomes [9,10]. Loss of chromosome 22 and/or heterozygous deletion of *SMARCB1*, while it has been reported, is a rare event in conventional axial chordoma [9,32]. In the study by Tarpey et al [10], out of 104 cases, there was a single case designated as extra-axial chordoma (3rd finger), which did not show mutations or copy number alternations by targeted Next-Generation Sequencing analysis.

Poorly differentiated variant of chordoma is a tumor of pediatric and young adult age group, commonly occurring at clivus/cervical vertebral location and is pathologically characterized by sheets of epithelioid cells with eosinophilic cytoplasm, nuclear atypia and loss of INI-1 expression due to inactivating mutations and/or recurrent isolated copy number losses involving *SMARCB1* at 22q11.23 [5-7]. In a prior case report of a conventional chordoma from the sacrum with transformation to poorly differentiated chordoma, we showed that *SMARCB1* loss (homozygous) may be an early event in rare cases of axial conventional chordoma and a poorly differentiated chordoma can evolve through additional genomic aberrations such as doubling of the genome [39]. Extra-axial poorly differentiated chordoma is exceptionally rare with a single published case report of a 67-year-old female who presented with a knee mass with destruction of the medial cortex of metadiaphysis of distal femur and a large extraosseous soft tissue mass[21].

As chordomas in general belong to the C-class group, we utilized a genome-wide high-resolution single nucleotide polymorphism (SNP)-Array and/or fluorescence in situ hybridization (FISH) to analyze copy number changes and allelic imbalances in the 6 extra-axial chordoma cases. In addition next-generation sequencing (MSK-IMPACT) results were available for 3 patients and in all cases we could confirm deletion of *SMARCB1.*

Our results showed that the genetics features of extra-axial conventional chordoma align with alterations observed in poorly differentiated axial chordoma. Our three cases with extra-axial conventional chordomas in this study showed only a few genomic imbalances, with consistent loss of chromosome 22 or a focal deletion involving the *SMARCB1* gene at 22q11.2. In our case number 6 with both conventional and poorly differentiated chordoma components, we found heterozygous deletion of *SMARCB1* in the conventional chordoma

component without additional genetic alterations. Similar to our previous case report of axial poorly differentiated chordoma [39], the extra-axial poorly differentiated chordomas (2 cases) demonstrated a complex hyperdiploid genomic profile with gain of multiple chromosomes and a homozygous deletion of *SMARCB1*. No mutations or structural variants were identified in all three extra-axial chordomas with available NGS-targeted sequencing analysis (MSK-IMPACT). The finding of ch22 loss and/or heterozygous deletion of *SMARCB1* in 5/6 cases suggest that this is a crucial genetic alteration in extra-axial chordomas. In this small series, we did not find any evidence of chromothripsis, unlike conventional chordoma.

INI1 protein, encoded by *SMARCB1* gene, is a core subunit of an ATP-dependent chromatin remodeling complex-SWI/SNF that plays an important role in maintaining genome stability and preventing tumorigenesis [40]. The loss of INI1 expression due to homozygous deletion of *SMARCB1* was known to be associated with a number of tumors including epithelioid sarcoma, myoepithelial carcinoma, epithelioid malignant peripheral nerve sheath tumor, and malignant rhabdoid tumor [41]. In the present study, we observed the loss of INI1 expression in both conventional and poorly differentiated components of the extra-axial poorly differentiated chordoma where the conventional component showed only focal heterozygous deletion of 22q including *SMARCB1* focus. The loss of INI1 expression in the conventional component might be due to the decreased *SMARCB1* mRNA expression secondary to heterozygous deletion of *SMARCB1*. In a study of whole genome sequencing of 91 cases of clival chordoma, there was reduced mRNA levels in cases with heterozygous deletion of *SMARCB1* [37]. In another study [40] it was shown that heterozygous deletion of *SMARCB1* led to a significant down-regulation of *SMARCB1* mRNA expression in Gastrointestinal Stromal Tumors (GISTs). Other unexplored epigenetic mechanisms affecting the unaltered allele is another alternative possibility. One of our conventional chordoma cases (case number 4) showed partial loss of INI1 by immunohistochemistry despite no deletion of *SMARCB1* detected by FISH analysis. This was a biopsy material and the partial loss of INI1 could be related to the decalcification. In the four cases involving bone, our pancytokeratin showed patchy positivity which is likely related decalcification effect as our two soft tissue extra-axial chordomas showed expected diffuse positivity.

Currently, the preferred treatment for patients with extra-axial chordoma is resection with wide margins and there is no evidence of benefit from radiotherapy or chemotherapy. In our series, three of four extra-axial conventional chordoma patients had local recurrence. All three recurrent cases were initially treated with curettage. No recurrence was seen in the resected case with negative margins. In follow-up of these cases (32-174 months), none has recurred or metastasized. In contrast, both extra-axial poorly differentiated chordoma patients developed distant metastases.

SMARCB1 gene deletion in the pathological development of 83% of the cases of extra-axial chordoma is a novel finding. The inactivation of *SMARCB1* is believed to cause oncogenesis through the loss of inhibition of Enhancer of Zeste homologue 2 (EZH2) which is a catalytic subunit of the PRC2 polycomb repressive complex whose overexpression leads to oncogenesis [42]. Therefore, EZH2-targeting agents have been shown to induce tumor regression and radiation sensitivity in models of malignant rhabdoid tumor, and

a novel EZH2 inhibitor, Tazemetostat, has entered clinical trials for patients with INI1-deficient tumors including poorly differentiated chordoma, malignant rhabdoid tumor, and epithelioid sarcoma (Clinicaltrials.gov NCT02601937 and NCT02601950) [43-46]. There was also a recent report of partial response in the primary site and complete response in the metastatic lung nodules in a young patient with a poorly differentiated chordoma, who received treatment with Tazemetostat in a phase II clinical trial followed by radiation to the primary site [47]. Whether there may be benefit from EZH2 inhibitors in patients with metastatic poorly differentiated extra-axial chordomas cannot be determined based on single case report but can be speculated.

In conclusion, we found that in this small series, extra-axial conventional chordoma shows consistent loss of ch22 and/or heterozygous deletion of *SMARCB1* gene without the additional copy number genetic alternations described in axial conventional chordomas. We were able to show in one of the two poorly differentiated extra-axial chordoma cases, the phenotypic progression was accompanied by homozygous deletion of *SMARCB1* with genome complexity and hyperdiploidy. The possibility of *SMARCB1* deletion as a driver gene event in extra-axial chordoma needs analysis of a larger number of cases.

Funding

This research is supported by the National Cancer Institute (NCI) of the National Institute of Health (NIH) (P30 CA008748).

Data availability statement

The data that support the findings of this study are available from the corresponding author upon reasonable request.

References

1. Heffelfinger MJ, Dahlin DC, MacCarty CS, Beabout JW. Chordomas and cartilaginous tumors at the skull base. Cancer. 1973;32(2):410–420. [PubMed: 4722921]
2. WHO Classification of Tumours Editorial Board e. WHO Classification of Tumours 5th Edition: Soft Tissue and Bone Tumours. Geneva: WHO Press. 2020.
3. O'Donnell P, Tirabosco R, Vujovic S, et al. Diagnosing an extra-axial chordoma of the proximal tibia with the help of brachyury, a molecule required for notochordal differentiation. Skeletal Radiol. 2007;36(1):59–65. [PubMed: 16810540]
4. Vujovic S, Henderson S, Presneau N, et al. Brachyury, a crucial regulator of notochordal development, is a novel biomarker for chordomas. J Pathol. 2006;209(2):157–165. [PubMed: 16538613]
5. Shih AR, Cote GM, Chebib I, et al. Clinicopathologic characteristics of poorly differentiated chordoma. Mod Pathol. 2018;31(8):1237–1245. [PubMed: 29483606]
6. Hasselblatt M, Thomas C, Hovestadt V, et al. Poorly differentiated chordoma with SMARCB1/INI1 loss: a distinct molecular entity with dismal prognosis. Acta Neuropathol. 2016;132(1):149–151. [PubMed: 27067307]
7. Hoch BL, Nielsen GP, Liebsch NJ, Rosenberg AE. Base of skull chordomas in children and adolescents: a clinicopathologic study of 73 cases. Am J Surg Pathol. 2006;30(7):811–818. [PubMed: 16819322]
8. Le LP, Nielsen GP, Rosenberg AE, et al. Recurrent chromosomal copy number alterations in sporadic chordomas. PLoS One. 2011;6(5):e18846. [PubMed: 21602918]

9. Wang L, Zehir A, Nafa K, et al. Genomic aberrations frequently alter chromatin regulatory genes in chordoma. Genes Chromosomes Cancer. 2016;55(7):591–600. [PubMed: 27072194]
10. Tarpey PS, Behjati S, Young MD, et al. The driver landscape of sporadic chordoma. Nature communications. 2017;8(1):890.
11. Zhu GG, Ramirez D, Chen W, et al. Chromosome 3p loss of heterozygosity and reduced expression of H3K36me3 correlate with longer relapse-free survival in sacral conventional chordoma. Hum Pathol. 2020;104:73–83. [PubMed: 32795465]
12. Lantos JE, Agaram NP, Healey JH, Hwang S. Recurrent skeletal extra-axial chordoma confirmed with brachyury: imaging features and review of the literature. Skeletal Radiol. 2013;42(10):1451–1459. [PubMed: 23653219]
13. Cheng DT, Mitchell TN, Zehir A, et al. Memorial Sloan Kettering-Integrated Mutation Profiling of Actionable Cancer Targets (MSK-IMPACT): A Hybridization Capture-Based Next-Generation Sequencing Clinical Assay for Solid Tumor Molecular Oncology. The Journal of molecular diagnostics : JMD. 2015;17(3):251–264. [PubMed: 25801821]
14. Ali S, Leng B, Reinus WR, Khilko N, Khurana JS. Parachordoma/myoepithelioma. Skeletal Radiol. 2013;42(3):431, 457–438. [PubMed: 22618759]
15. Tirabosco R, Mangham DC, Rosenberg AE, et al. Brachyury expression in extra-axial skeletal and soft tissue chordomas: a marker that distinguishes chordoma from mixed tumor/myoepithelioma/parachordoma in soft tissue. Am J Surg Pathol. 2008;32(4):572–580. [PubMed: 18301055]
16. Neumann J, Gersing AS, Barth TF, Boxberg M, Woertler K. Intra-articular extra-axial chordoma of the wrist: a case report with review of the current literature. Skeletal Radiol. 2019;48(12):2015–2020. [PubMed: 31104146]
17. Bitzer A, McCarthy EF, Morris CD. Extra-Axial Chordoma of the Hand. J Hand Surg Am. 2017;42(11):933 e931–933 e935. [PubMed: 28709789]
18. Ueda T, Kubota K, Shiroma N, et al. Extra-axial chordoma of the gingiva. Auris Nasus Larynx. 2020;47(2):299–304. [PubMed: 30904199]
19. Tsukamoto S, Vanel D, Righi A, Donati DM, Errani C. Parosteal extra-axial chordoma of the second metacarpal bone: a case report with literature review. Skeletal Radiol. 2018;47(4):579–585. [PubMed: 29151144]
20. Kurzawa P, Fundowicz M, Dopierala M, Larque AB, Nielsen GP. Primary extra-axial, para-articular chordoma of the knee. A case report and the review of literature. Histopathology. 2018;72(5):883–885. [PubMed: 29156101]
21. Balogh P, O'Donnell P, Lindsay D, Amary MF, Flanagan AM, Tirabosco R. Extra-axial skeletal poorly differentiated chordoma: a case report. Histopathology. 2020;76(6):924–927. [PubMed: 31880336]
22. DiFrancesco LM, Davanzo Castillo CA, Temple WJ. Extra-axial chordoma. Arch Pathol Lab Med. 2006;130(12):1871–1874. [PubMed: 17149966]
23. Primary Rekhi B., large extra-axial chordoma in proximal tibia: a rare case report with literature review and diagnostic implications. APMIS. 2016;124(3):238–242. [PubMed: 26522887]
24. Holley C, Breining T, Scheithauer M, Moller P, Barth TFE. [Primary extra-axial chondroid chordoma of the anterior nasal septum: case report of a rare chordoma with literature review]. HNO. 2020.
25. Suzuki H, Yamashiro K, Takeda H, Nojima T, Usui M. Extra-axial soft tissue chordoma of wrist. Pathol Res Pract. 2011;207(5):327–331. [PubMed: 21397407]
26. DeComas AM, Penfornis P, Harris MR, Meyer MS, Pochampally RR. Derivation and characterization of an extra-axial chordoma cell line (EACH-1) from a scapular tumor. J Bone Joint Surg Am. 2010;92(5):1231–1240. [PubMed: 20439670]
27. Huang J, Bhojwani N, Oakley FD, Jordanov MI. Proximal tibial extra-axial chordoma masquerading as renal cell carcinoma metastasis. Skeletal Radiol. 2017;46(11):1567–1573. [PubMed: 28702752]
28. Park SY, Kim SR, Choe YH, et al. Extra-axial chordoma presenting as a lung mass. Respiration. 2009;77(2):219–223. [PubMed: 18497501]
29. Righi A, Sbaraglia M, Gambarotti M, et al. Extra-axial chordoma: a clinicopathologic analysis of six cases. Virchows Arch. 2018;472(6):1015–1020. [PubMed: 29560513]

30. Tihy F, Scott P, Russo P, Champagne M, Tabet JC, Lemieux N. Cytogenetic analysis of a parachordoma. Cancer Genet Cytogenet. 1998;105(1):14–19. [PubMed: 9689924]

31. Rinner B, Weinhaeusel A, Lohberger B, et al. Chordoma characterization of significant changes of the DNA methylation pattern. PLoS One. 2013;8(3):e56609. [PubMed: 23533570]

32. Choy E, MacConaill LE, Cote GM, et al. Genotyping cancer-associated genes in chordoma identifies mutations in oncogenes and areas of chromosomal loss involving CDKN2A, PTEN, and SMARCB1. PLoS One. 2014;9:e101283. [PubMed: 24983247]

33. Kelley MJ, Korczak JF, Sheridan E, Yang X, Goldstein AM, Parry DM. Familial chordoma, a tumor of notochordal remnants, is linked to chromosome 7q33. Am J Hum Genet. 2001;69(2):454–460. [PubMed: 11452362]

34. Yang X, Beerman M, Bergen AW, et al. Corroboration of a familial chordoma locus on chromosome 7q and evidence of genetic heterogeneity using single nucleotide polymorphisms (SNPs). Int J Cancer. 2005;116(3):487–491. [PubMed: 15818627]

35. Yang XR, Ng D, Alcorta DA, et al. T (brachyury) gene duplication confers major susceptibility to familial chordoma. Nat Genet. 2009;41(11):1176–1178. [PubMed: 19801981]

36. Ciriello G, Miller ML, Aksoy BA, Senbabaoglu Y, Schultz N, Sander C. Emerging landscape of oncogenic signatures across human cancers. Nat Genet. 2013;45(10):1127–1133. [PubMed: 24071851]

37. Bai J, Shi J, Li C, et al. Whole genome sequencing of skull-base chordoma reveals genomic alterations associated with recurrence and chordoma-specific survival. Nat Commun. 2021;12(1):757. [PubMed: 33536423]

38. Cottone L, Eden N, Usher I, et al. Frequent alterations in p16/CDKN2A identified by immunohistochemistry and FISH in chordoma. J Pathol Clin Res. 2020;6(2):113–123. [PubMed: 31916407]

39. Curcio C, Cimera R, Aryeequaye R, et al. Poorly differentiated chordoma with whole-genome doubling evolving from a SMARCB1-deficient conventional chordoma: A case report. Genes Chromosomes Cancer. 2021;60(1):43–48. [PubMed: 32920865]

40. Bracken AP, Brien GL, Verrijzer CP. Dangerous liaisons: interplay between SWI/SNF, NuRD, and Polycomb in chromatin regulation and cancer. Genes Dev. 2019;33(15-16):936–959. [PubMed: 31123059]

41. Kohashi K, Oda Y. Oncogenic roles of SMARCB1/INI1 and its deficient tumors. Cancer Sci. 2017;108(4):547–552. [PubMed: 28109176]

42. Wilson BG, Wang X, Shen X, et al. Epigenetic antagonism between polycomb and SWI/SNF complexes during oncogenic transformation. Cancer Cell. 2010;18(4):316–328. [PubMed: 20951942]

43. Alimova I, Birks DK, Harris PS, et al. Inhibition of EZH2 suppresses self-renewal and induces radiation sensitivity in atypical rhabdoid teratoid tumor cells. Neuro Oncol. 2013;15(2):149–160. [PubMed: 23190500]

44. Knutson SK, Warholic NM, Wigle TJ, et al. Durable tumor regression in genetically altered malignant rhabdoid tumors by inhibition of methyltransferase EZH2. Proc Natl Acad Sci U S A. 2013;110(19):7922–7927. [PubMed: 23620515]

45. Chi SN MG, Hoffman L, Macy M, Doleman S, Blakemore SJ, et al. A phase I study of the EZH2 inhibitor tazemetostat in pediatric subjects with relapsed or refractory INI1-negative tumors or synovial sarcoma. J Clin Oncol. 2016;34(15):TPS10587.

46. Stacchiotti S SP, Jones R, Agulnik M, Villalobos VM, Jahan TM, et al. Safety and efficacy of tazemetostat, a first-in-class EZH2 inhibitor, in patients (pts) with epithelioid sarcoma (ES) (NCT02601950). J Clin Oncol. 2019;37(15):11003.

47. Gounder MM, Zhu G, Roshal L, et al. Immunologic Correlates of the Abscopal Effect in a SMARCB1/INI1-negative Poorly Differentiated Chordoma after EZH2 Inhibition and Radiotherapy. Clin Cancer Res. 2019;25(7):2064–2071. [PubMed: 30642912]

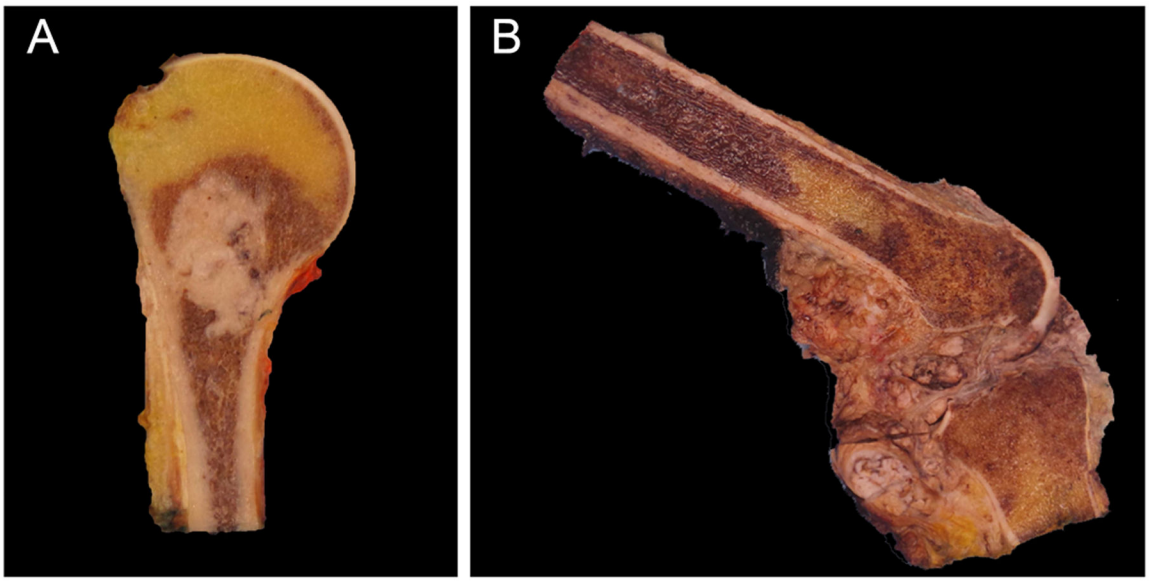

Figure 1:
(A) Case 1. Gross photograph of humeral head reveals a well-circumscribed lobulated white tumor with fleshy cut surface in the right humeral neck. (B) Case 6. Gross photograph of the left knee en-bloc resection specimen along the coronal plane reveals a large mass involving deep soft tissues within the femoral tibial joint and interchondylar notch, with white tan, nodular, solid to focal myxoid cut surface. Focal necrosis and hemorrhage are noted.

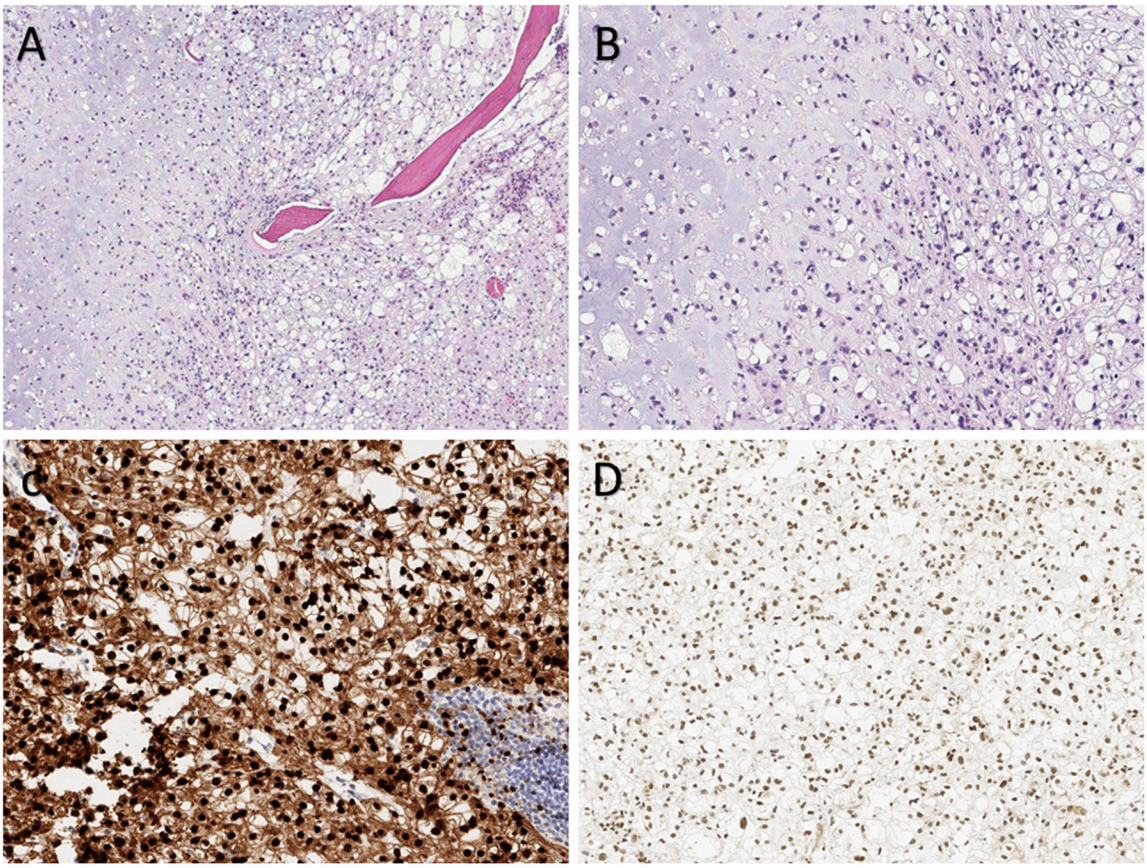

Figure 2:

Case 1. Photomicrograph showing epithelioid cells with variably vacuolated clear to eosinophilic cytoplasm in an abundant extracellular myxoid matrix, infiltrating the trabecular bone (H&E, A x 100 magnification; B x 200 magnification). There is minimal to mild cytologic atypia without mitosis and necrosis. Immunohistochemical analysis shows that the tumor cells have diffusely strong nuclear positivity for brachyury (C x 200 magnification) and have retained nuclear expression of INI-1 protein (D x 200 magnification).

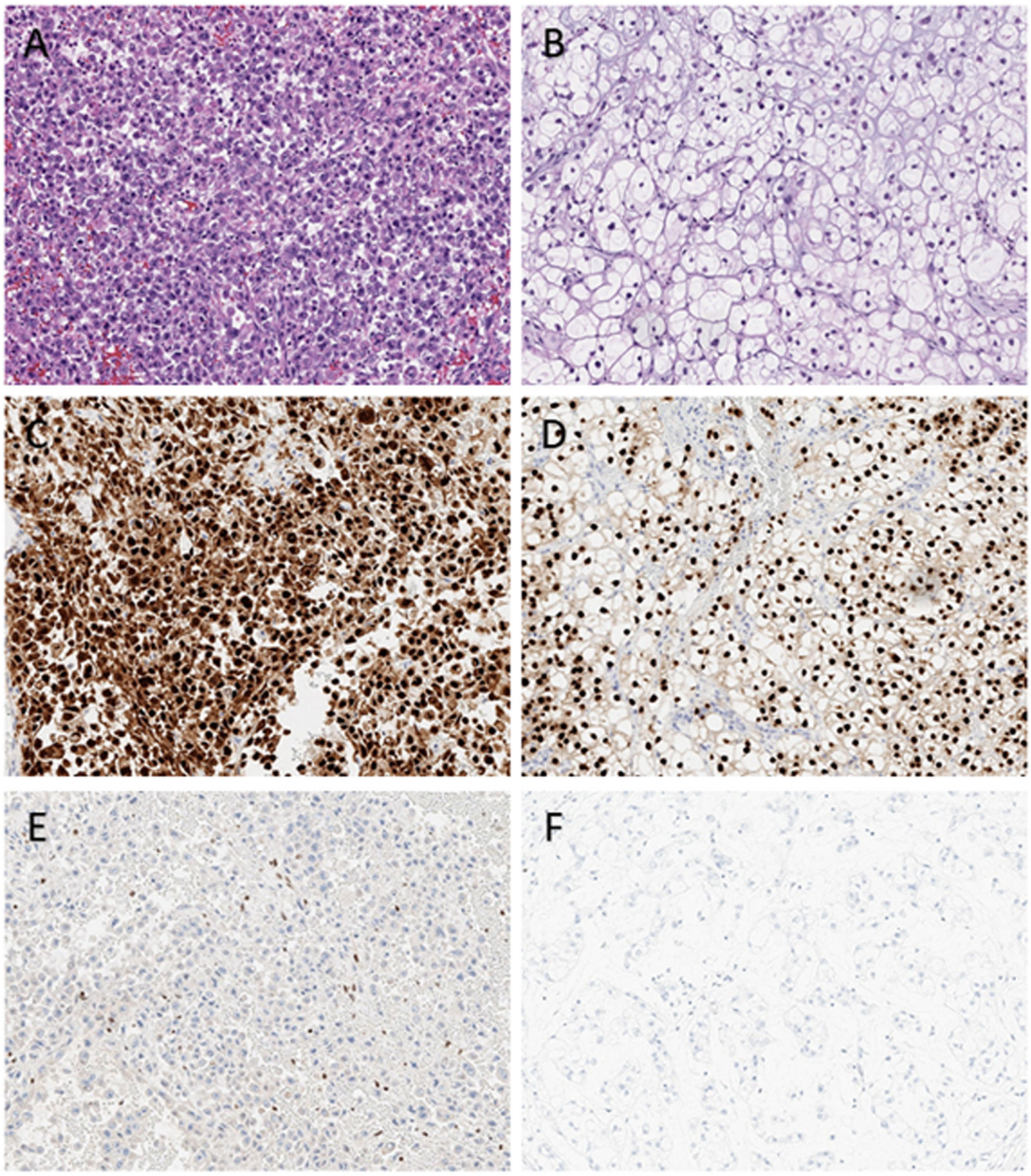

Figure 3:

Case 6. Photomicrograph of the poorly differentiated component showing solid sheets of poorly differentiated epithelioid to rhabdoid cells with nuclear pleomorphism, prominent nucleoli and abundant eosinophilic cytoplasm without an extracellular myxoid stroma (H&E, A x 200 magnification). The conventional component shows more well differentiated epithelioid cells with partially vacuolated clear to eosinophilic cytoplasm organized in cords or nests in an abundant extracellular myxoid matrix (H&E, B x 200 magnification). Diffuse immunoreactivity for brachyury is present in both the poorly differentiated (C x 200 magnification), and conventional (D x 200 magnification) components. There is uniform

loss of INI-1 nuclear expression in both the poorly differentiated (E x 200 magnification) and conventional (F x 200 magnification) components.

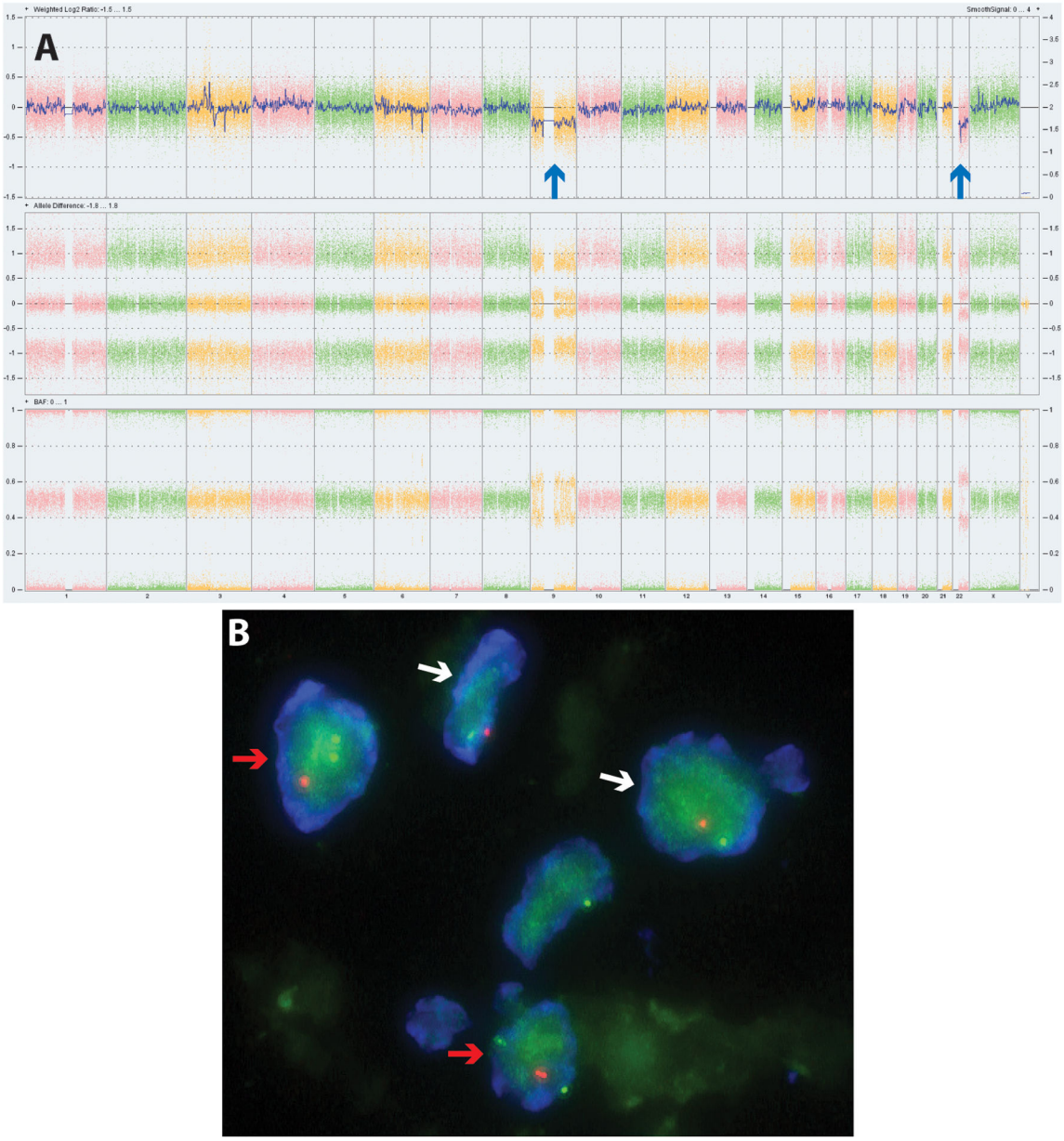

Figure 4:

Case 1. OncoScan SNP array and FISH on the extra-axial conventional chordoma. (A) OncoScan SNP array revealed loss of chromosomes 9 and 22 (blue arrows, top row), supported by allele differences and B allele frequencies (bottom two rows); (B) FISH result showing heterozygous loss of *SMARCB1* (orange) along with the internal control (green) in two cells (white arrows) and two cells (red arrow) with a heterozygous deletion of *SMARCB1* (orange) and retained two copies of the internal control (green). Many cells show loss of both signals due to loss of chromosome 22.

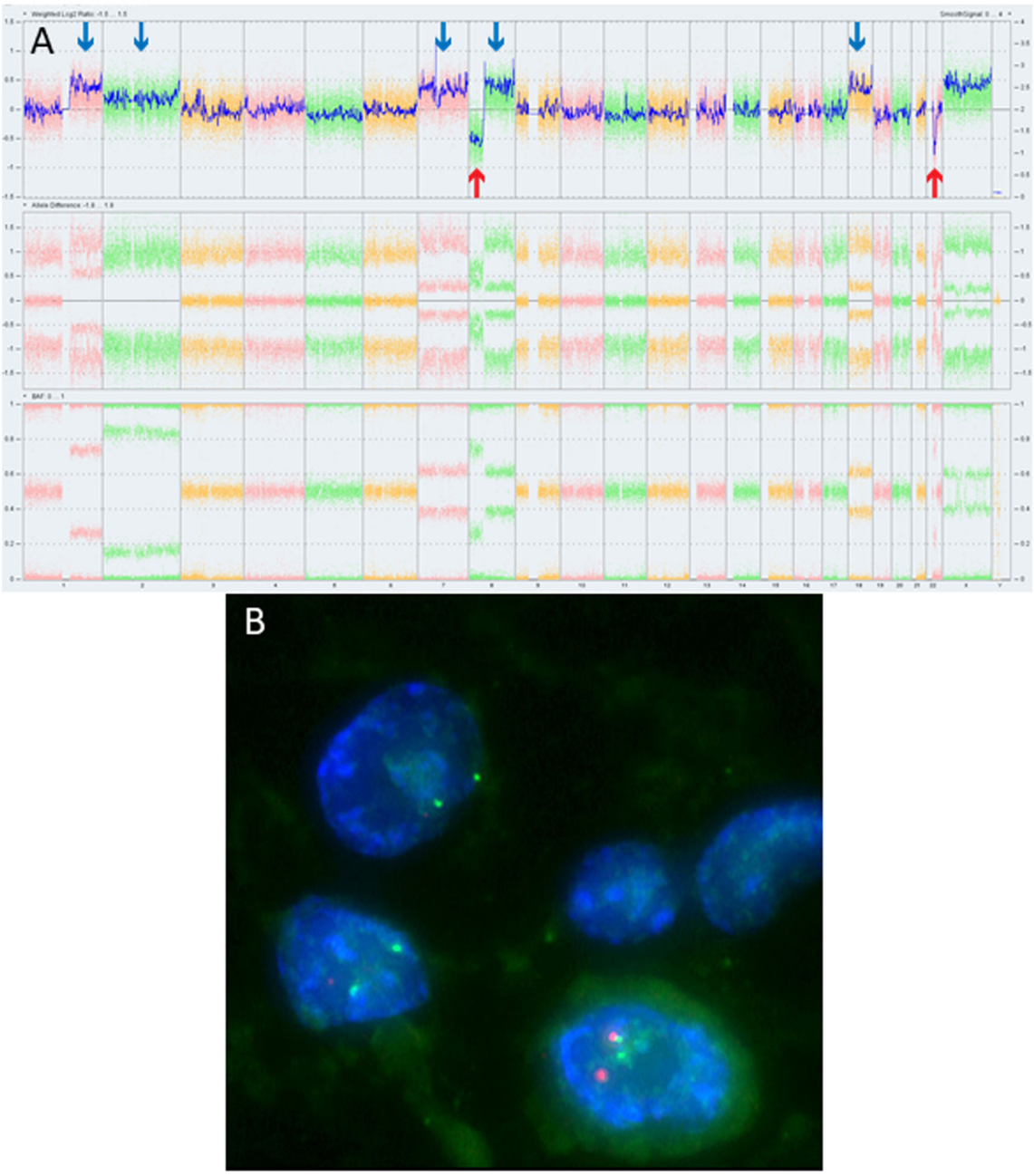

Figure 5:

Case 5. OncoScan SNP array and FISH on the extra-axial poorly differentiated chordoma. (A) OncoScan SNP array revealed complex genomic imbalances with gain of chromosomes or chromosomal arms 1q, 7, 8q, and 18, CN-LOH of chromosome 2 (blue arrows, top row) and loss of 8p and segment 22q11.21-q12.2(red arrows, top row) which includes *SMARCB1* and supported by allele differences (bottom rows). (B) FISH result of the poorly differentiated component shows homozygous deletion of *SMARCB1* with retained two internal control signals (green) and no signal of *SMARCB1.* A normal cell displays two signals each for the control probe (green) and *SMARCB1* (orange).

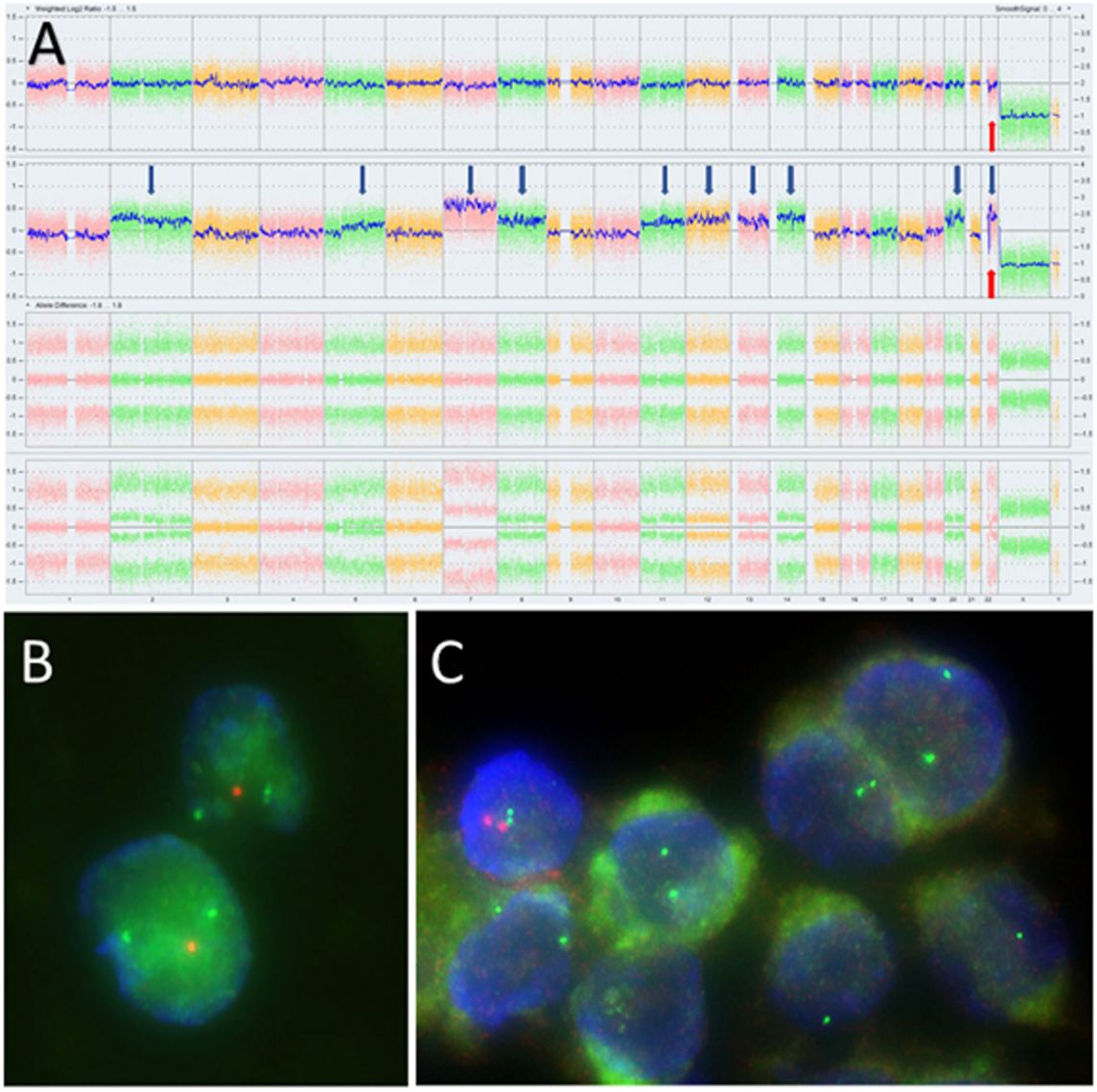

Figure 6:

Case 6. OncoScan SNP array and FISH on the extra-axial poorly differentiated chordoma. (A) OncoScan SNP array revealed a low level deletion of 22q11.2, including the *SMARCB1* gene in conventional component (red arrow, top row). The poorly differentiated component showed complex genomic imbalances including gain of chromosomes or chromosomal arms 2, 5q, 7, 8, 11, 12, 13, 14, 20 and 22 (blue arrows, second row), and homozygous deletion of the *SMARCB1* gene (red arrow, second row), supported by allele differences (bottom rows). (B) FISH result of the conventional component shows a heterozygous deletion of *SMARCB1* (orange) with retained two copies of the internal control (green). (C) FISH result of the poorly differentiated component shows homozygous deletion of *SMARCB1* with retained two internal control signals (green) and no signal of *SMARCB1*. A normal cell displays two signals each for the control probe (green) and *SMARCB1* (orange).

Table 1

Clinicopathological features of six cases of extra-axial chordoma

Case	Age/sex	Clinical symptom(s)	Site	Location	Size	Radiographic features	Treatment	Local recurrence	Mets	Follow-up
1	54/F	Shoulder pain	Right proximal humerus	Intra-medullary	3.7 cm	Lytic lesion	Radical resection	No	No	32 months
2	30/F	Finger swelling	Middle phalynx of right index finger	Intra-medullary	1.5 cm	Lytic lesion	Excision/curettage, Ray resection of the finger	Yes (2.5 years)	No	84 months
3	21/F	Leg pain	Right distal tibia	Intra-cortical	3.4 cm	Lytic lesion	Excision/curettage, Radical resection	Yes (8 months)	No	144 months
4	21/F	Knee pain	Left distal femur	Intra-cortical	5.1 cm	Lytic lesion	Excision/curettage x 2	Yes (2 years)	No	174 months
5	21/F	Elbow pain	Left elbow	Intra-articular	7.8 cm	STM with calcifications, bone erosion	Chemotherapy	n/a	Yes	7 months
6	52/M	Knee pain and swelling	Left knee	Intra-articular	15.4 cm	STM with calcifications, no bone erosion	Radical resection, chemotherapy, radiation	No	Yes	21 months

Abbreviations: STM, soft tissue mass; Mets, metastases; case number 3&4-previously published (12)

Table 2

INI1 IHC, SNP array and FISH results of 6 cases of extra-axial chordoma

Case	Subtype of Extra-axial chordoma	INI-1 IHC	SNP array results	FISH results- *SMARCB1*
1	Conventional	Retained	Loss of ch9, 22, and focal deletion involving the *SMARCB1* gene at 22q11.2	Heterozygous deletion
2	Conventional	Retained	Loss of ch22, gain of 4q, and focal deletion involving the *SMARCB1* gene at 22q11.2	Heterozygous deletion
3	Conventional	Retained	n/a	Heterozygous deletion
4	Conventional	P-retained	n/a	Heterozygous or homozygous deletion not detected
5	Poorly differentiated with conventional component	Loss in both components	Gain of ch1q, 7, 8q, and 18, CN-LOH of chromosome 2 and loss of 8p and segment 22q11.21-q12.2.	Homozygous deletion (poorly differentiated component only)
6	Poorly differentiated with conventional component	Loss in both components	Focal deletion involving the *SMARCB1* gene at 22q11.2 (conventional component)	Heterozygous deletion (conventional component)
			Gain of ch2, 5q, 7, 8, 11, 12, 13, 14, 20 and 22, and homozygous deletion of the *SMARCB1* gene (poorly differentiated component)	Homozygous deletion (poorly differentiated component)

Abbreviations: P-retained, partially retained; n/a, not available; ch, chromosome